Vol 13 No 4, April 2004
1009-1963/2004/13(04)/0505-05

Chinese Physics

© 2004 Chin. Phys. Soc.
and IOP Publishing Ltd

Experimental investigation of the impact on nearby solid boundary during laser-generated bubble collapse*

Chen Xiao(陈 笑), Xu Rong-Qing(徐荣青), Shen Zhong-Hua(沈中华),
Lu Jian(陆 建), and Ni Xiao-Wu(倪晓武)†

Department of Applied Physics, Nanjing University of Science & Technology, Nanjing 210094, *China*

(Received 16 July 2003; revised manuscript received 27 October 2003)

Cavitation damage has been considered as being responsible for many effects in hydraulic machinery and biological medicine. In order to better understand the cavity interaction with nearby solid surfaces, the impact loading induced by the high-speed liquid-jet and subsequent jet flow during the final stage of the bubble collapse in a static fluid is investigated by focusing a Q-switched pulsed laser into water. By means of a new method based on a fibre-coupling optical beam deflection technique, a detailed experimental study has been made to clarify the relationship of the impact pressure against a solid boundary as a function of the dimensionless γ that is generally used to describe the bubble dynamics with its definition $\gamma = s/R_{\max}$ ($R_{\max}$ being the maximum bubble radius and s denoting the distance of the cavity inception from the boundary). The experimental results are shown that for γ in the range of about 0.67 to 0.95 with a pulsed laser energy 230mJ, the transient pressure applied on the solid surface is maximum; while for $\gamma > 1$ or $\gamma < 0.67$, it is gradually decreased. By combination of our experimental results with the other work that detected the acoustic emission during the bubble collapse at different γ, it is concluded that in this range of 0.67–0.95, the destructive effect due to a liquid-jet and the following jet flow impact actually outweighs the well-known effect of shock wave emission and plays a vital role during the cavitation bubble collapse.

Keywords: optical beam deflection, laser-generated bubble, liquid-jet, cavitation
PACC: 4762, 4755B

1. Introduction

Cavitation was first observed as the damage of the great ocean liners' propellers after a surprisingly small time in use, which then raised people's interest to investigate the destructive cause. [1] Nowadays, this phenomenon has been widely studied in many fields at home and abroad. [2–6] For example, in the field of hydraulic machinery or materials science, for the solid metallic surfaces, cavity interaction is erosive, leaving, at best, the surfaces pock-marked. In medical application, such as intraocular laser surgery, pulsed laser can produce both intended beneficial medical effects and undesirable collateral effects. So how to maximize the medical benefit while keep damage to a minimum is an important subject. Cavitation is also important in nuclear reactors where the acoustic effects associated with cavitation can act as a diagnostic tool for observing the onset of heat transfer faults in a coolant system.

Cavitation bubbles usually appear wherever the pressure change occurs in hydraulic machinery, such as in pump or propeller where flow is disturbed and wherever temperature effects lead to vapour cavities. At present, the techniques for the cavity generation include a kinetic impulse,[7] spark discharge [8] and pulsed-laser generation.[9] Among them, laser-produced cavitation bubbles offer excellent possibilities for studying the bubble dynamics in model experiment because they can be made highly spherical, free from mechanical distortion and easy to control.

When a cavitation bubble is in the vicinity of a solid boundary, during the final stage of its collapse, the most striking feature is the formation of a high-speed, wall-directed reentrant jet from the bubble sur-

*Project supported by the National Natural Science Foundation of China (Grant No 60208004), the Natural Science Foundation of Jiangsu Province (Grant No BK2001056), the Teaching and Research Award Program for Outstanding Young Professor in Higher Education Institute, Ministry of Education, China and the National Key Opening Experimental Foundation of Laser Technology (Grant No 2005).

†Corresponding author. Tel:(025)84315699, Fax:(025)84315019, E-mail: nxw@mail.njust.edu.cn

face farthest from the wall associated with the emission of shock wave. It hits the opposite bubble wall from the inside and induces an intense impact against the boundary. In most cases, the bubble may undergo several oscillations near the boundary, which may induce the secondary liquid-jets and shock waves emission. The whole interaction process was first observed by means of a high-speed photographic technique in 1975.[10] Recent investigations have shown that the dynamical behaviour of a single bubble and the jet formation is closely dependent on the dimensionless distance $\gamma = s/R_{\max}$ with $R_{\max}$ being the maximum bubble radius and s denoting the distance of a laser focus (the point of bubble inception) from a solid boundary as shown in Fig.1.[2−4,9,11] A bubble with different $R_{\max}$ but the same γ value exhibits similar dynamics.[4] Although recent works on bubble dynamics are reported by different authors, the behaviour of a bubble near the boundary is still not thoroughly understood, especially for the final collapse stage.

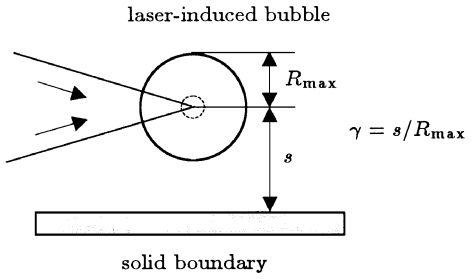


Fig.1. Geometrical relations for the definition of the parameter γ.

In the experiment aspect, there are many detection techniques, including high-speed photographic technique, Schlieren imaging, PVDF pressure transducer, probe beam deflection, etc. But some of them are very complex, difficult to adjust or high cost. In this paper, we propose a new detection technique based on fibre-coupling optical beam deflection (OBD). This detection technique is very simple and effective. The whole setup is compact and easy to adjust. Furthermore, it can provide the temporal development of the impulse pressure, whereas the others, such as the high-speed photography, cannot. By this method, we have presented the stress experienced by a solid boundary as a function of the nondimensional γ when the laser-induced cavitation bubble oscillates in its vicinity. All results lead to the conclusion that at laser energy 230mJ, γ in the range of about 0.67 to 0.95, the impact on the solid surface, which is induced by the combination of the liquid-jet impact and the subsequent jet flow, is the maximum. So in this range, the destructive effect due to liquid-jet impact and the following jet flow outweighs the well-known effect of shock waves and plays a vital role in the cavitation bubble collapse.

2. Experiment

The experimental arrangement for investigations the relationship between the nondimensional γ and the pressure against a solid boundary induced by the laser bubble collapse in its vicinity is outlined in Fig.2. A single bubble is generated in the cuvette filled with distilled water by using a Q-switched Nd:YAG laser (wavelength 1.06μm, pulse width 30ns, pulsed energy up to 650mJ) after the laser pulse is expanded and collimated. Here the laser beam is selected to focus parallel, not perpendicular to the flat face of the solid material. Take into consideration that in the experiment the point of laser focus cannot be distinguished well, so that the distance between the location of the bubble inception and the wall is difficult to define because the laser focus is generally elongated in the incident direction of the laser due to small impurities present and several spots of optical breakdown in the focal region.

In the detection region, a He–Ne laser as a probe source (wavelength 0.63μm, output power 5mW) is focused by an aspherical lens (f_1=30mm) used for eliminating the spherical aberration. In order to detect the transient impact, the probe beam is focused on the bare polished rear-face of the material at the epicentre. Here the target material is selected to be 10mm-diam, 0.25mm-thick cleanly polished iron plate, which is stuck previously in the cuvette wall (100nm× 500nm×150mm) as shown in Fig.2. The reflected beam is focused by a microscope objective (f_2=4mm) into a single-mode optical fibre that is mounted on a five-axis fibre-regulating-stand with a spatial resolution 0.1μm. The output beam from the fibre is put into photomultiplier (Hamamatsu 5773 with 2ns rise time) and displayed on a digital oscilloscope (Tektronix 730A, 1Gs/s). A part of the scattered laser beam is fed into a PIN photodiode with 0.1ns rise time to generate the trigger signal. In order to increase the signal-to-noise ratio, a narrow-band filter is used before the reflected beam is coupled into the fibre. Here, the numbers 8, 9, 10, 11, 12 and 13 as shown in Fig.2 build up a subsystem, called an OBD testing system. To a certain degree, it is similar to the

knife-edge method in basic principles because both of them obtain the information by detecting the reflected beam deflection. But receiver elements and detailed measurement principles are quite different.

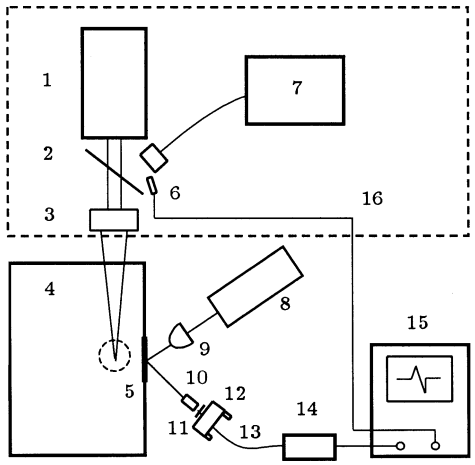


Fig.2. Schematic of experimental arrangement: 1. Q-switched Nd:YAG laser, 2. beam splitter, 3. expanding–collimating lens, 4. optical-glass cuvette, 5. iron plate, 6. PIN photodiode, 7. energy probe, 8. He-Ne laser, 9. aspherical lens, 10. microscope objective, 11. interference filter, 12. 5-axis fibre-regulating-stand, 13. single-mode optical fibre, 14. photomultiplier, 15. digital oscilloscope, 16. platform.

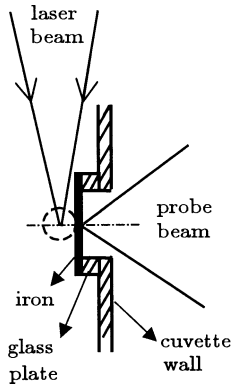


Fig.3. Enlarged view of detection part.

In order to adjust the distance between laser focus and the boundary, we use a platform with the minimum movement distance 10μm. It can control synchronously the movements of Nd: YAG laser, beam splitter, expansion–collimation setup, energy-probe and PIN photodiode in the direction perpendicular to the iron plate surface. Consider that at a relatively small distance to the boundary, a laser pulse will be partly blocked by the cuvette wall. We additionally stuck between the iron plate and cuvette wall a 30mm-diam, 5mm-thick glass-plate with a round hole in the center as shown in Fig.3. In this experiment, the incident laser energies are 80mJ and 230mJ. The movement range of the laser focus to the solid boundary is from 0.5mm to 2.6mm.

3. Results and discussion

Figure 4 displays the pressure spikes for a laser-generated cavity interacting with an iron boundary in water at the incident laser energy 230mJ. The distance s, from the laser focus to the boundary is 0.8mm. In this figure, there exist two obvious spikes 'a' and 'b'. Taking into account the cuvette size, we eliminate the possibility that signal 'b' is the echo of spike 'a' from the cuvette wall. The relative amplitude of peak 'a' is higher than that of 'b' with their time interval 42μs. Since the pulsed laser in this experiment is parallel to, not perpendicular to, the iron plate, so the laser-induced plasma ablation effects on the iron surface are excluded. In this experiment, we consider that spikes 'a' and 'b' actually correspond to the pressure signals around the first and second minimum volumes of cavitation bubble, respectively. Pressure spike 'a' is induced by the liquid-jet impact and the subsequent jet flow lasting 20μs after the first bubble collapse, while spike 'b' is produced by the secondary liquid-jet and the following water flow when the bubble re-expands and then collapses until it finally dissolves in water. Besides the main peaks, there are also some smaller signals we cannot explain clearly.

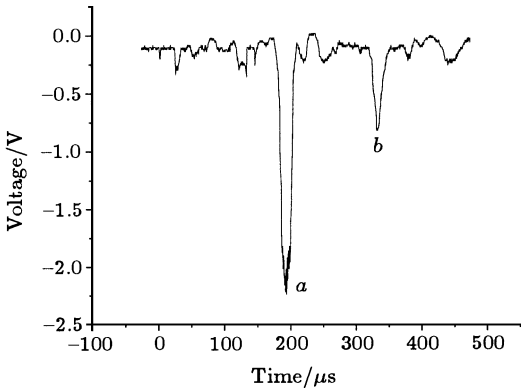


Fig.4. Typical signal at the distance 0.8mm from the bubble inception to the solid boundary at laser energy 230mJ.

Here we are interested in spike 'a' only, because it has the most relevance to potential damage processes. Spike 'a' appears at the time of 192μs. Besides, under the same energy radiation, this dominant loading pressure occurs approximately at the same time with the fluctuation about 5μs, although at a different distance. It is also observed that the time of pressure

occurrence is increased with the laser energy. For an incident laser energy 80mJ, the first peak occurs at 124μs, whereas at energy 230mJ, it is at 192μs.

The Rayleigh expression of the maximum bubble radius for a spherical bubble collapse is as follows:[12]

$$R_{\max} = T_{\rm c} \Big/ \left[0.915 \left(\frac{\rho}{p_{\rm stant} - p_{\rm v}}\right)^{0.5}\right], \qquad (1)$$

where ρ is the density of the liquid, $p_{\rm stant}$ the static pressure, $p_{\rm v}$ the vapour pressure of a liquid, $T_{\rm c}$ is the bubble collapse duration. The above equation states that the bubble maximum radius is determined by its collapse duration and the corresponding pressure gradient. Lauterborn[13] has demonstrated that expansion and collapse of laser-induced bubbles are highly symmetric, if the laser pulse duration is much shorter than the oscillation period of the bubble, and if the viscosity of the liquid is small. So the time interval between the bubble inception and collapse is twice the collapse duration. Therefore, according to the definition $\gamma = s/R_{\max}$, the relationship between the pressure loading on the boundary and the dimensionless γ can be obtained. The values used in Eq.1 are given in Table 1.

Table 1. The values of parameters employed in Eq.1.

E/mJ	ρ/(kg/m^3)	$p_{\rm stant}$/Pa	$p_{\rm v}$/Pa (20°C)	$T_{\rm c}/\mu$s	$R_{\max}$/mm
80	1000	100000	2330	62	0.67
230	1000	100000	2330	96	1.04

In Fig.5, each point is the average of five experimental data. Consider that the distance from the laser focus to the solid boundary ranges from 0.5mm to 2.6mm, then the corresponding γ will vary from 0.48 to 2.5 at laser energy 230mJ; while at 80mJ the corresponding γ is from 0.74 to 3.9.

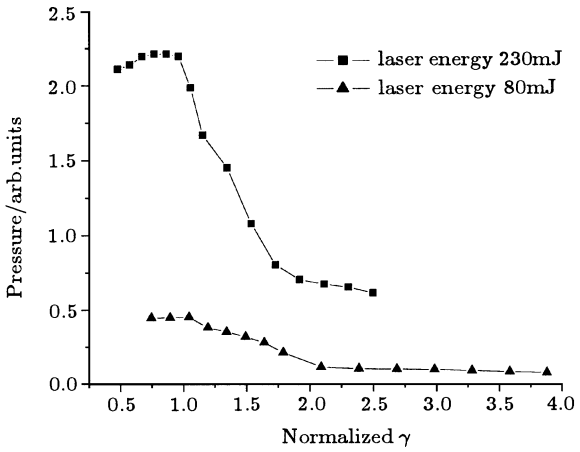


Fig.5. Pressure detected at the epicentre as a function of the normalized γ during the laser-induced bubble collapse near the solid boundary.

At the energy 230mJ, γ in the range from 0.67 to 0.96, the pressures loaded have the maximum values; while for $\gamma > 0.95$ or $\gamma < 0.67$, their amplitude are decreased. At 80mJ, when $\gamma > 1.04$, the amplitudes are also decreased, but there are obviously slower than those with the laser energy 230mJ. For $\gamma > 1$, there is a water layer between the bubble and boundary, which weakens the jet impact and the subsequent jet flow, so that pressures against the boundary are greatly reduced. For larger γ, the main signal is gradually diminished until the liquid-jet does not emerge any more. But when the bubble is generated close to the boundary, i.e. $\gamma < 1$, there is no water-damping layer so that the liquid-jet impact is higher than that in the case with $\gamma > 1$. The bubble dynamics are influenced more by the boundary condition. During the last stage of collapse, the jet-induced vortex ring (one of general feature of the bubble collapse near the boundary) is formed, which takes a part of the energy from the kinetic energy of radial flow into the bubble. Hence, the bubble content becomes less compressed than that in the case of large γ value. Vogel and Lauterborn[14] have pointed out that at $\gamma = 0.9$ the energy of acoustic emission is the minimum. So in this range, the destructive factor induced by the liquid-jet impact and jet flow pressure outweighs, in effect, the acoustic waves, while for $\gamma < 0.67$, in the case of energy 230mJ, the detected signal is a little decreased. From the pictures taken by high-speed photography, for $\gamma = 0.34$ with the maximum bubble radius $R_{\max}$=2.3mm,[15] the shape of the bubble is nearly hemispherical and it hardly moves. So the bubble is more like spherical collapse and the acoustic wave becomes intense again, leading to the increase of acoustic energy converted from the total bubble energy. Therefore, the kinetic energy of the liquid-jet transformed from the bubble energy is a little decreased compared with that of $0.67 \le \gamma \le 0.95$. For $0.67 \le \gamma \le 0.95$, the high-speed liquid-jet impact and the following jet flow against the boundary outweigh, in effect, the implosion mechanism and play a main role in destructive mechanisms.

4. Conclusion

A new method based on fibre-coupling OBD technique is presented in this paper. Compared with the other techniques, it is simple, effective and easy to adjust. It offers a new possibility for the study of the temporal development of transient pressure loading on the nearby boundary. By using this technique, the mechanical effects during laser-induced bubble collapse in the vicinity of a solid boundary are investigated. The experimental results reveal that during the collapse stage, the nearby target material is affected by two impacts in turn: one is generated by liquid-jet impact and the subsequent jet flow that last about 20μs during the single bubble first collapse; the other is produced by secondary liquid-jet and the following water flow during the bubble rebound period. The amplitude as well as the lifetime of the former is larger than that of the latter. Furthermore, the relationship between the impact pressure and the dimensionless γ is investigated in detail. When pulsed laser energy is 230mJ, in the range of $0.67 \leq \gamma \leq 0.95$, the first pressure against the solid boundary generated by liquid-jet and subsequent jet flow has the maximum value; while $\gamma > 0.95$ or $\gamma < 0.67$, this impact is decreased. Then according to Ref.[14], at $\gamma = 0.9$ the acoustic effect during the bubble collapse is the minimum. Hence, in this range, the liquid-jet and jet flow outweigh, in effect, the well-known acoustic emission by a collapsing bubble at the minimum volume and play a main role in destructive action.

References

[1] Silberrad D 1912 *Propeller erosion, Engineering* pp33–35

[2] Tomita Y and Shima A 1986 *J. Fluid Mech.* **169** 535

[3] Vogel A, Schweiger P, Frieser A, Asiyo M N and Birngruber R 1990 *IEEE J. Quant. Electron.* **26** 2240

[4] Ohl C D, Kurz T, Geisler R, Lindau O and Lauterborn W 1999 *Phil. Trans. R. Soc. Lond.* A **357** 269

[5] He Y S, Liu H and Zhao G 1997 *Acta Mech. Sin.* **29** 1

[6] Jiang G J, Lin J H, Ma J and Zhao J P 1998 *Acta Acustica* **23** 401

[7] Benjamin T B and Ellis A T 1966 *Phil. Trans. R. Soc. London Ser.* A **260** 221

[8] Blake J R and Gibson D C 1981 *J. Fluid Mech.* **170** 479

[9] Schiffers W P, Shaw S J and Emmony D C 1998 *Ultrasonics* **36** 559

[10] Lauterborn W and Bolle H 1975 *J. Fluid Mech.* **72** 391

[11] Philipp A and Lauterborn W 1998 *J. Fuild. Mech.* **361** 75

[12] Rayleigh Lord. 1917 *Phil. Mag.* **34** 94

[13] Lauterborn W 1974 *Acustica* **31**51

[14] Vogel A and Lauterborn W 1988 *J. Acoust. Soc. Am.* **84** 719

[15] Vogel A, Lauterborn W and Timm R 1989 *J. Fluid Mech.* **206** 299